4D imaging of crack evolution and failure mode in 3DP rock-like samples under uniaxial compression by using in-situ micro-ct technology

Yulong Shao
Seoul National University, Seoul, Korea

Jineon Kim
Seoul National University, Seoul, Korea

Jae-Joon Song
Seoul National University, Seoul, Korea

ABSTRACT: Previous studies have investigated static cracks and pores before and after compressive tests of 3D-printed (3DP) rock with limitations in describing real-time cracking and damage evolution during compression. In this study, compression tests were conducted on 3DP gypsum rocks using an in-situ micro-computed tomography (micro-CT) system to obtain 2D CT images during compression. Through 3D reconstruction of 2D CT images, crack propagation and pore evolution of 3DP gypsum rocks could be illustrated from a 3D stereoscopic perspective and quantitatively analyzed. Results indicated that multiple tensile cracks propagated along the axial direction during compression. Initially, the volume of 3DP gypsum rocks decreased owing to pore closure during the compaction stage in which cracks were yet to be initiated. As the external stress exceeded the bearing capacity of 3DP gypsum rocks, the crack volume increased first marginally and then rapidly as cracks initiated and further developed with the increased stress.

Keywords: 3DP gypsum rocks, in-situ micro-CT, 3D reconstruction, crack propagation, pore evolution.

1 INTRODUCTION

Three-dimensional (3D) printing is an emerging technology that has garnered increasing interest in the rock mechanics community as it is controllable, repeatable, accurate, efficient, time-saving, and economical (Fereshtenejad & Song 2016, Ishutov 2019 and Kong et al. 2021). It allows researchers to prepare identical specimens, replicate complex structures, and visualize the interior of intact rocks, creating new possibilities for understanding rock mechanics (Gao et al. 2021, Jiang & Zhao 2015 and Ju et al. 2014). Various mechanical tests have been conducted on 3DP rock-like samples using various printing materials—including resin, acrylonitrile butadiene styrene, polylactic acid, cement, gypsum, and sand powder—to examine whether 3D printing technology can be applied to rock mechanics (Fereshtenejad & Song 2016, Ishutov 2019, Kong et al. 2021, Gao et al. 2021, Jiang & Zhao 2015, Ju et al. 2014, Song et al. 2022 and Zhu et al. 2018).

X-ray micro-computed tomography (micro-CT) is an effective nondestructive method for identifying and visualizing the interior structures of rocks in 3D. In several rock-engineering studies,

this technique has been used to analyze the microstructural properties and the extent of damage in natural rocks (Yao et al. 2009 and Duliu 1999). By combining 3D printing and micro-CT technologies, high-precision results can be obtained with repeated sample preparation of natural rocks (Zhu et al. 2018 and Song et al. 2022), and the pore structure and crack morphology of 3DP samples can also be analyzed and quantified (Kong et al. 2018 and Zhu et al. 2018). However, only a few studies have investigated the crack propagation and pore evolution of 3DP rock-like samples under compressive tests using in-situ micro-CT technology, which is essential for characterizing and understanding the failure mechanism and microstructural evolution of 3DP rock-like samples for modeling natural rock behavior.

In this study, 3D-printed (3DP) cylindrical gypsum samples of size Φ 7.5 × 15 mm were subjected to uniaxial compressive tests using an in-situ micro-CT system equipped with a loading apparatus. 2D CT images were captured at different stages of compression, and 3D models of the interior of the 3DP sample were reconstructed at each stage. Based on the 3D reconstructions, the crack propagation and pore structure evolution of the 3DP gypsum rocks were quantitatively analyzed and characterized. The findings of this study can help characterize and understand the damage evolution and microstructural changes in 3DP gypsum rocks under compressive loading.

2 EXPERIMENT AND METHODS

2.1 3D printer and sample preparation

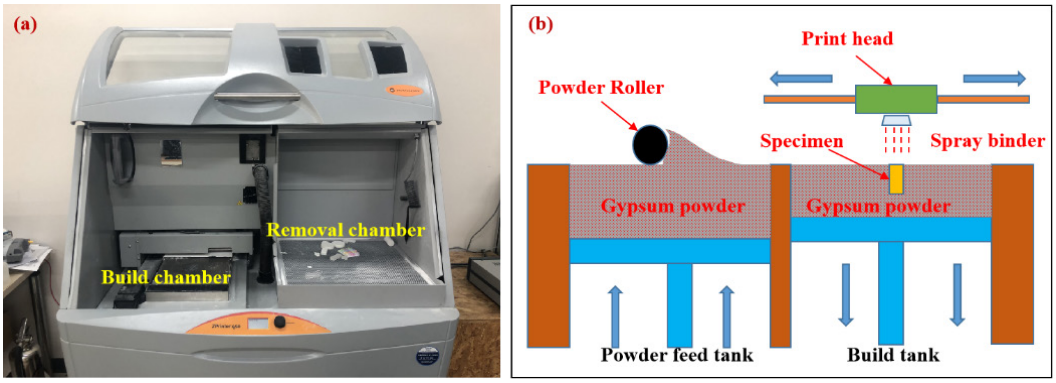

Figure 1. Schematic of ZPrinter450 (a) and its printing mechanism (b).

A ZPrinter450 manufactured by 3D Systems Corporation) was used to generate three cylindrical samples of size Φ 7.5 × 15 mm by the layer-by-layer additive manufacturing of gypsum powder based on a digital model, as shown in Figure 1(a). The printing mechanism of ZPrinter450 is illustrated in Figure 1(b). First, the powder feed tank is moved upward, and the build bed is automatically filled with gypsum powder. A roller is then used to spread a thin layer of predetermined thickness over the build bed as the build tank moves downward, providing a smooth surface for the sample. Next, a computer-controlled print head sprays the binder onto the gypsum powder. When the first layer is completed, the build bed descends to prepare for the next layer. Several repetitions of this cycle are performed to construct the entire physical model.

In this study, a layer thickness of 0.1 mm and a binder saturation level of 100% were adopted for sample preparation. Before the *in*-situ micro-CT scanning tests, all samples were maintained at a constant temperature of 20 °C and a humidity of 60% for 7 days.

2.2 In-situ micro-CT uniaxial compression system

The in-situ micro-CT uniaxial compression system used in this study comprised a commercial Skyscan Material Testing Stage installed inside a Skyscan 1272 micro-CT, as shown in Figure 2(a). Figure 2(b) illustrates the working mechanism of the in-situ micro-CT compression system,

comprising three parts—that is, an X-ray source, an X-ray detector, and a detachable loading apparatus. First, the X-rays generated by the X-ray source are transmitted to the target sample, and those that penetrate the sample are recorded by an X-ray detector on the other side as 2D projection images. Next, the sample is rotated in small fractions using the rotational stage, and X-ray projection images are captured at different angles. These steps are repeated until a full turn of 360° is achieved. The obtained 2D cross-sectional images are computationally reconstructed to generate a 3D model of the sample interior.

In this study, the sample was rotated by 360° in steps of 0.3°, and an X-ray image was captured with an exposure time of 5000 ms after each rotation. Constant displacement loading was performed with a loading rate of 4 μm/s for all tests. At each scanning step, a total of 1500 images were captured at an image resolution of 10 μm for the 3D reconstruction and subsequent quantitative analysis of the cracking and microstructural evolution. The crack propagation and pore evolution were analyzed through image processing, which included image cropping, background denoising, Gaussian filtering, image binarization, image reconstruction, and microstructure analysis, using Avizo and ImageJ software. The shape factor was adapted as a criterion to distinguish cracks and pores, as prior studies have used geometric segmentation techniques to distinguish them based on their relative shapes (Landis 2005 and Sun et al. 2022).

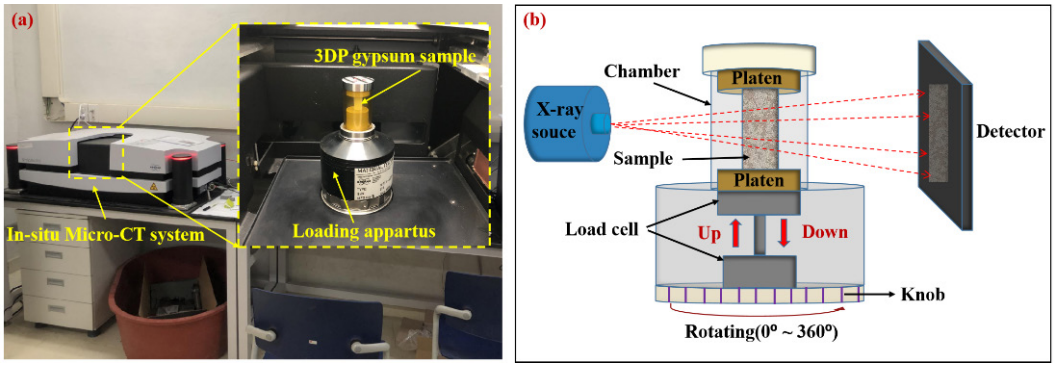

Figure 2. Schematic of the in-situ micro-CT compression system (a) and its working mechanism (b).

3 RESULTS AND DISCUSSION

3.1 Mechanical properties and scanning steps

In this study, three 3DP gypsum samples were subjected to uniaxial compression tests with and without CT scanning, as shown in Figure 3. Two samples were subjected to uniaxial compression tests without CT scanning to obtain the full stress-strain curve and validate the mechanical consistency of the 3DP gypsum samples, as shown in Figure 3(a). The sample responses illustrate that the mechanical properties of the 3DP gypsum samples are consistent. Moreover, the stress-strain curves of the 3DP gypsum samples can be characterized by four stages—that is, the compaction, elastic, plastic, and residual failure stages.

Figure 3(b) shows the stress-strain curve of the 3DP gypsum rock for which CT scans were conducted during uniaxial compression. Five CT scans were conducted at different stages of deformation to study crack propagation and pore evolution in the 3DP gypsum rocks. Notably, stress relaxation is evident at each scanning step because of the time required for CT imaging, which was approximately two hours (Duan et al. 2019).

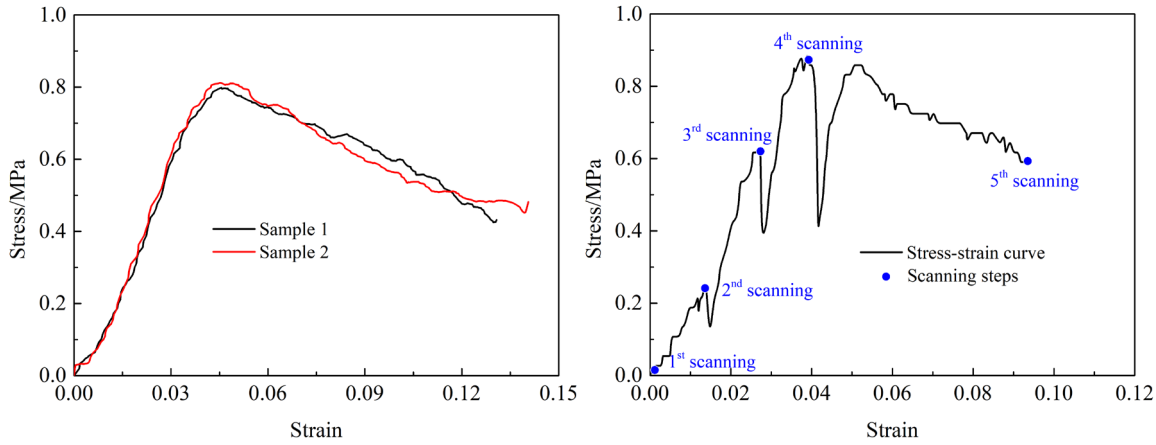

(a) (b)

Figure 3. The stress-strain curve without scanning (a) and the stress-strain curve with scanning (b), in which the blue points denote the CT scanning steps.

3.2 Crack propagation

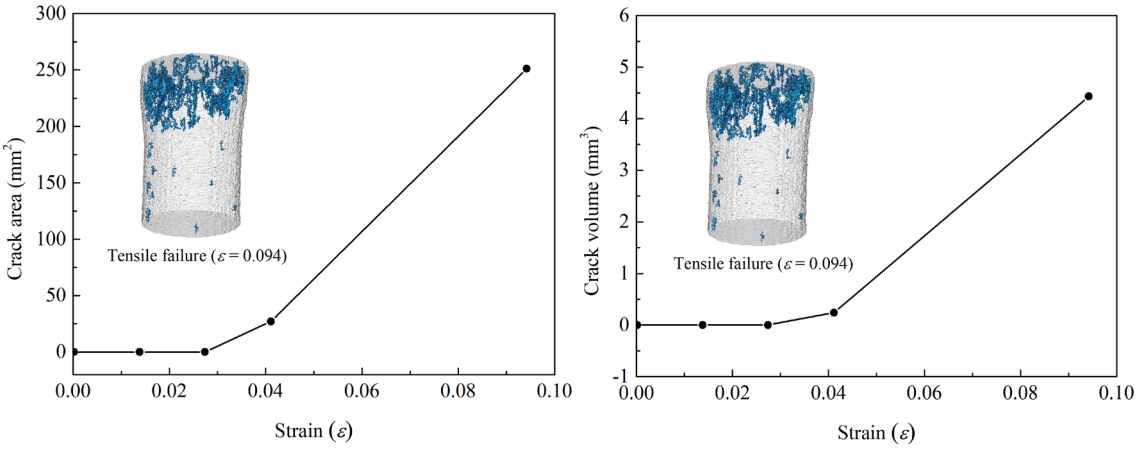

(a) Crack area (b) Crack volume

Figure 4. Evolution of 3D cracks inside the 3DP gypsum rock at different strains.

The crack distribution and evolution characteristics were analyzed by determining the crack area and volume during compression. Figures 4(a) and 4(b) show the evolution of the crack area and volume inside the 3DP gypsum rock. Combining the results shown in Figures 3 and 4, there are no cracks inside the 3DP gypsum rock during the compaction and elastic stages of the stress-strain curves. The load stress of the 3DP gypsum rock is low during the early stages ($\varepsilon < 0.0274$) so cracks are not initiated. When the 3DP gypsum rock enters the plastic stage ($0.0274 < \varepsilon < 0.0411$) as stress increases, the crack area and crack volume increase to 27.12 mm^2 and 0.24 mm^3, respectively, reflecting the crack initiation and growth. When the strain exceeds 0.0411, the crack growth and penetration result in substantial crack area and crack volume increments—specifically, 223.93 mm^2 in crack area and 4.19 mm^3 in crack volume. The crack distribution shows that tensile cracks form along the bedding planes of the 3DP gypsum rock, illustrating their mechanical anisotropy.

3.3 Pore evolution

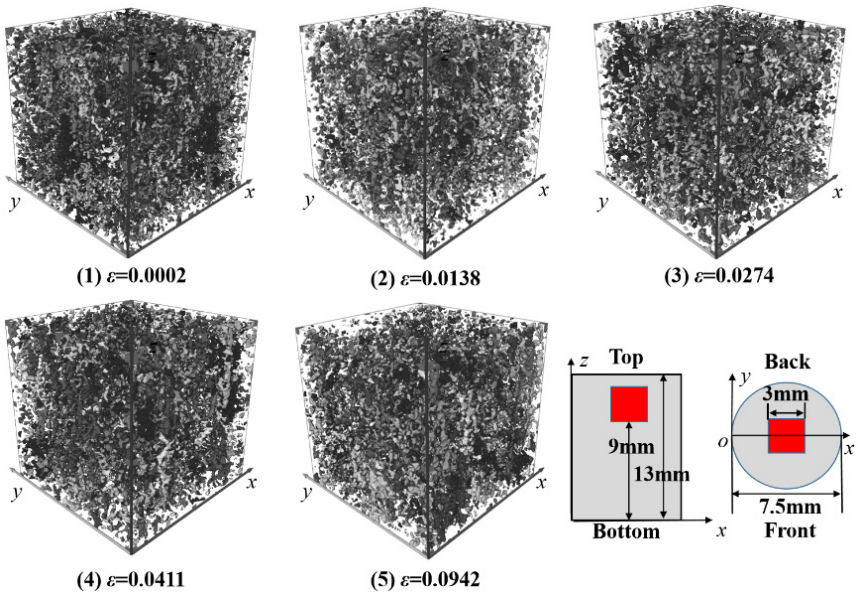

Figure 5. Evolution of 3D pores inside the 3DP gypsum rock at different strains.

A cubic region of interest (ROI) with the size of $3\times3\times3mm^3$ was selected to investigate the pore evolution of the 3DP gypsum rock during loading, as shown in Figure 5. To solely analyze the pore evolution of the 3DP gypsum rock at different stages of deformation, fractures were excluded from the ROI based on their geometric shape. The number of pores inside the 3DP gypsum rock first decrease and then increase during the remaining stages of compression. It is evident that only a portion of the pores is compressed and closes during the initial compaction stage ($\varepsilon < 0.0138$)—that is, pores inside the 3DP gypsum rock are compressed and close as depicted by the concave trend of the initial stress-strain curve. After pore closure and compression, the number of pores gradually increases as the strain increases in the elastic, plastic, and residual stages.

4 CONCLUSION

In this study, the crack propagation and pore evolution of 3DP gypsum rocks were investigated by conducting uniaxial compression tests using in-situ micro-CT technology. The stress-strain curves of the 3DP gypsum rocks could be divided into four stages—that is, the compaction, elastic, plastic, and residual failure stages. Based on 3D reconstruction of the 2D CT images during different stages, the internal structural evolution of the 3DP gypsum rock could be demonstrated from a stereoscopic perspective and quantitatively described. Crack initiation and growth within the 3DP gypsum rock occurred during the plastic stage, whereas no cracks were evident during the compaction or elastic stages. The crack area and volume initially increased first slowly and then rapidly as the strain increased. The pore volume decreased during the compaction stage and then increased during later stages.

ACKNOWLEDGEMENTS

This work was supported by Korea Institute of Energy Technology Evaluation and Planning (KETEP) grant funded by the Korea government (MOTIE) (20214000000500, Training program of CCUS for the green growth), and by the National Research Foundation of Korea (NRF) grant funded by the Korea government (MSIT) (No. 2022R1F1A1076409).

REFERENCES

Duan, Y.T., Li, X., Zheng, B., He, J.M., & Hao, J. 2019. Cracking Evolution and Failure Characteristics of Longmaxi Shale Under Uniaxial Compression Using Real-Time Computed Tomography Scanning. Rock Mechanics and Rock Engineering 52, pp. 3003-301. DOI: 10.1007/s00603-019-01765-0.

Duliu, O. G. 1999. "Computer axial tomography in geosciences: an overview." Earth-Science Reviews 48, pp. 265-281. DOI: 10.1016/S0012-8252(99)00056-2.

Fereshtenejad, S., & Song, J.J. 2016. Fundamental Study on Applicability of Powder-Based 3D Printer for Physical Modeling in Rock Mechanics. Rock Mechanics and Rock Engineering, 49, pp. 2065-2074. DOI: 10.1007/s00603-015-0904-x.

Gao, Y.T., Wu, T.H., & Zhou, Y. 2021. Application and prospective of 3D printing in rock mechanics: A review. International Journal of Minerals Metallurgy and Materials 28, pp. 1-17. DOI: 10.1007/s12613-020-2119-8.

Jiang, C., & Zhao, G.F. 2015. A Preliminary Study of 3D Printing on Rock Mechanics. Rock Mechanics and Rock Engineering 48, pp. 1041-1050. DOI: 10.1007/s00603-014-0612-y.

Ju, Y., Xie, H.P., Zheng, Z.M., Lu, J.B., Mao, L.T., Gao, F., & Peng, R.D. 2014. Visualization of the complex structure and stress field inside rock by means of 3D printing technology. Chinese Science Bulletin 59, pp. 5354-5365. DOI: 10.1007/s11434-014-0579-9.

Landis, E.N. 2005. Damage variables based on three-dimensional measurements of crack geometry. Strength, fracture and complexity 3, pp. 163-173.

Kong, L.Y., Ishutov, S., Hasiuk, F., & Xu, C.C. 2021. 3D Printing for Experiments in Petrophysics, Rock Physics, and Rock Mechanics: A Review. Spe Reservoir Evaluation & Engineering 24, pp. 721-732. DOI: https: 10.2118/206744-Pa.

Kong, L.Y., Ostadhassan, M., Li, C.X., & Tamimi, N. 2018. Can 3-D Printed Gypsum Samples Replicate Natural Rocks? An Experimental Study. Rock Mechanics and Rock Engineering 51, pp. 3061-3074. DOI: 10.1007/s00603-018-1520-3.

Sun, L.L., Zhang, C., Wang, G., Huang, Q.M., & Shi, Q. L. 2022. Research on the evolution of pore and fracture structures during spontaneous combustion of coal based on CT 3D reconstruction. Energy 260. ARTN 12503310.1016/j.energy.2022.125033.

Song, R., Wang, Y., Tang, Y., Peng, J.J., Liu, J.J., & Yang, C.H. 2022. 3D Printing of natural sandstone at pore scale and comparative analysis on micro-structure and single/two-phase flow properties. Energy 261. DOI: ARTN 12522610.1016/j.energy.2022.125226.

Yao, Y.B., Liu, D.M., Che, Y., Tang, D.Z., Tang, S.H., & Huang, W.H. 2009. Non-destructive characterization of coal samples from China using microfocus X-ray computed tomography. International Journal of Coal Geology 80, pp. 113-123. DOI: 10.1016/j.coal.2009.08.001.

Zhu, J.B., Zhou, T., Liao, Z.Y., Sun, L., Li, X.B., & Chen, R. 2018. Replication of internal defects and investigation of mechanical and fracture behaviour of rock using 3D printing and 3D numerical methods in combination with X-ray computerized tomography. International Journal of Rock Mechanics and Mining Sciences 106, pp. 198-212. DOI: 10.1016/j.ijrmms.2018.04.022.